Turk J Phys
27 (2003) , 459 – 479.

Quantum State Generation and Entanglement Manipulation Using Linear Optics

Şahin Kaya ÖZDEMİR, Takashi YAMAMOTO, Masato KOASHI
CREST Research Team for Interacting Carrier Electronics,
The Graduate University for Advanced Studies (SOKENDAI), Hayama, Kanagawa 240-0193, Japan
Nobuyuki IMOTO
CREST Research Team for Interacting Carrier Electronics,
The Graduate University for Advanced Studies (SOKENDAI), Hayama, Kanagawa 240-0193, Japan
NTT Basic Research Laboratories, 3-1 Morinosato Wakamiya, Atsugi, Kanagawa 243-0198, Japan

Received 08.09.2003

Abstract

Quantum information processing (QIP) requires unitary operations, measurements and synthesis, manipulation and characterization of arbitrary quantum states. Linear optics provides efficient tools for these purposes. In this review paper, we introduce the elements of linear optics toolbox, and briefly discuss some experimental and theoretical investigations using this toolbox. Our main focus will be the qubit state generation and entanglement extraction using linear optics toolbox.

Key Words: linear optics, quantum state, entanglement manipulation

1. Introduction

In recent years, the quantum engineering of light states has received much attention. This is mainly motivated by the potential improvement offered by quantum mechanics to the manipulation and the transmission of information. Quantum optics, which provides models some of which have been experimentally realized, plays an important role in this exploration. A quantum optics toolbox (QOT) for quantum information processing should contain elements which will enable the manipulation and coupling on single quanta level (photons, atoms) as well as on large ensembles and systems. Once the information is encoded on these quanta and systems, one needs quantum computing which includes tasks of manipulation and storage of information. Therefore, a QOT should include quantum gates, which might be implemented either using linear or non-linear optical components, and quantum memory for which there are candidates such as use of atomic ensembles, cold atoms and solid state based devices. Another important task in QIT is the transfer of the quantum and classical information between spatially separated parties. This requires channels which should not alter the characteristic and the nature of the information being sent through, that is, it should be damping and dissipation free. However, it is impossible to separate a quantum system from its surrounding; therefore dissipation and damping are unavoidable due to the coupling of the system with the environment. Then one should include elements which can decrease the effect of damping on their system and enough tools to recover the lost information partially or completely, if the system has been effected. And finally a QOT should include readout devices such as photon counting devices and schemes, as well as reconstruction schemes such as homodyne tomography.

The implementation of qubits, which are the quantum analog of classical bits, by photons opens a way to manipulate the represented information and transport it through free space or optical fibers. The

problem in photonic implementation shows itself in the operations where nonlinear effects are needed. This is beacuse at the single photon level the use of nonlinear effects is beyond the capabilities of the current photonic technology. However, the interference phenomenon, which can be observed by mixing photonic modes using linear optical elements and conditional dynamics together with photon counting, can create the required nonlinear effect for some implementations. Therefore, the investigation of the linear optical devices to understand what can be and what cannot be done using such devices is very crucial because of the direct relation to simple physical implementations. The benefit is that linear optical schemes are much easier to implement experimentally than the schemes which uses nonlinear media, but the drawback is that the nonlinearities induced by linear optical elements and measurement are less versatile and the success rate can be quite low especially when efficient photon counters and/or counting schemes are not available.

Recent theoretical and experimental studies have shown that linear optics toolbox (LOT) gives researchers enough number of tools to explore the quantum information processing technologies based on optical states of light. LOT has been proven to be ideal for the experimental implementation of several QIP protocols such as quantum teleportation [1] and quantum dense coding [2]. Although, these studies have started an excitement in the field, further studies revealed that linear optics have some limitations due not only to the intrinsic properties of the tools but also to the measurement devices used in the implementations.

Linear optics toolbox consists of photon counters, auxiliary photons, and simple but powerful components such as beamsplitters, polarization rotators and phase shifters. A survey of literature reveals that there is a high number of theoretical proposals of QIT implementations using this toolbox and there has been a tremendous effort in their experimental realizations covering a wide range from generation and manipulation of non-classical states of light to entanglement purification (a remedy to damping problem in quantum channels) and quantum gate constructions. Despite this encouraging studies, researchers have started to ask the question whether all stages of QIP is realizable solely using LOT or not and how the elements of this toolbox is related to the performance of these QIP implementations.

The purpose of this review paper is to introduce the linear optics toolbox, to discuss its limitations using the theoretical proposals and experimental realizations which have been presented in the literature. The paper is organized in six sections. In Sec. 2, the elements of the linear optics toolbox is briefly introduced. Sections 3 and 4 cover a discussion and review of the schemes proposed and experimentally realized for qubit state and Bell state preparation and measurement. In Sec. 5, entanglement manipulation protocols are introduced and realization of one of these protocols by our group using linear optics toolbox is explained in detail. Finally, Sec. 6 will be the conclusions.

2. Quantum state preparation using linear optics toolbox

In this section, we will briefly introduce the main elements of the linear optics toolbox and then describe some of the proposals and experiments performed for quantum state preparation.

2.1. Linear optics toolbox

The widely used elements of the linear optics toolbox can be listed as beamsplitters, phase shifters, photon counters, and auxiliary photons.

2.1.1. Beamsplitters

A beamsplitter (BS) is a two-input two-output device which channels the fields in the input modes, described by the operators $\hat{a}$ and $\hat{b}$, to the output modes, $\hat{c}$ and $\hat{d}$. Assuming a lossless and symmetric BS, the annihilation operators of the output modes are written as

$$\hat{c} = \hat{R}\hat{a}\hat{R}^{\dagger} \quad , \quad \hat{d} = \hat{R}\hat{b}\hat{R}^{\dagger} \tag{1}$$

where the beam splitter operator is [3]

$$\hat{R} = \exp\left[\theta(\hat{a}^{\dagger}\hat{b} - \hat{a}\hat{b}^{\dagger})\right] \tag{2}$$

with the amplitude reflection and transmission coefficients expressed, respectively, as $t = \cos\theta$ and $r = \sin\theta$. Suppose that input states are two independent Fock states, $|m,n\rangle \equiv |m\rangle_a|n\rangle_b$. The outputs are then a superposition of two-mode Fock states:

$$\begin{aligned}\hat{R}|m,n\rangle &= \sum_{j,k=0}^{m,n} \sqrt{\frac{(j+k)!(m+n-j-k)!}{m!n!}} \binom{m}{j}\binom{n}{k} \\ &\times(-1)^k(\cos\theta)^{n+j-k}(\sin\theta)^{m-j+k}|j+k, m+n-j-k\rangle \\ &= \sum_{j,k=0}^{m,n} R_{m,n}^{x,N-x}|x,N-x\rangle,\end{aligned} \tag{3}$$

where we have defined $x = j + k$, and the total number of input photons is $N = m + n$. Using Eq. 3, some basic properties of BS can be understood: (i) a beamsplitter can be used as an entangler. When the total number of input photons is N, the output state becomes an $(N+1)$-dimensional entangled state, i.e.,if $|m,n\rangle = |1,0\rangle$ then $\hat{R}|m,n\rangle = r|0,1\rangle + t|1,0\rangle$ which is a 2-dimensional entangled state. When $r = t = 1/\sqrt{2}$ that is a 50:50 BS ($\theta = \pi/4$), this state becomes a maximally entangled state of vacuum and one photon states. (ii) Amount of entanglement created at the output of BS can be found using the Von Neumann entropy of the reduced density operator which can be written as

$$E(\hat{\rho}_a) = -\sum_{j,k=0}^{m,n} |R_{m,n}^{x,N-x}|^2 \ln|R_{m,n}^{x,N-x}|^2. \tag{4}$$

Apparently, the amount of entanglement depends on the number of photons in the inputs and the reflection and transmission coefficients of the BS. For a maximally entangled state of $(N+1)$-dimension, $E(\hat{\rho}_a) = \ln(N+1)$. (iii) For a 50:50 BS, when $n = m$, it can be seen easily from Eq. 3 that all the terms where $j+k$ is an odd number cancel each other, and the terms obtained for even $j+k$ remain. Therefore, the term in the ket can be written as $|2x, 2n-2x\rangle$ which corresponds to states with even number of photons. The possibility of having states with odd number of photons is zero. This is due to the destructive interference of states with odd numbers. For example, for the input state $|1,1\rangle$, the output becomes $\hat{R}|1,1\rangle = [|0,2\rangle - |2,0\rangle]/\sqrt{2}$ which shows the channelling property of the 50:50 BS. When both inputs of the BS are coherent states, then we have $\hat{R}|\alpha_1,\alpha_2\rangle = |(r\alpha_1 + t\alpha_2),(t\alpha_1 + r\alpha_2)\rangle$ which is not an entangled state. Indeed, studies have shown that nonclassicality of at least one of the inputs is a necessary condition for the output of a BS to be entangled [4] .

2.1.2. Phase shifters

The action of a phase shifter acting on mode going through it is given by $\hat{P}_\phi = \mathrm{e}^{i\phi\hat{a}^\dagger\hat{a}}$ where $\hat{a}$ denotes the mode on which the phase shifter acts. If a Fock state of $|n\rangle$ passes through this phase shifter, the output state becomes $\mathrm{e}^{in\phi}|n\rangle$. As it is seen the induced phase shift is linearly proportional to the number of photons in that mode, i.e, $\hat{P}_\phi|0\rangle = |0\rangle$, $\hat{P}_\phi|1\rangle = \mathrm{e}^{i\phi}|1\rangle$, and $\hat{P}_\phi|2\rangle = \mathrm{e}^{i2\phi}|2\rangle$.

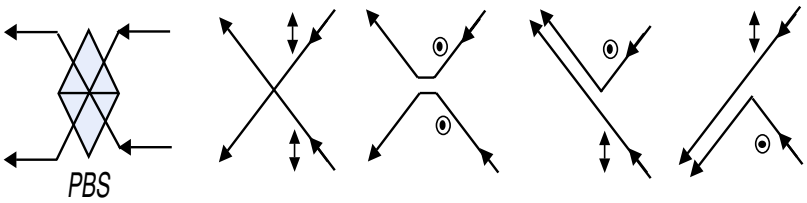

Figure 1. Schematic description of the input-output relation for a polarizing beam splitter (PBS). ↕ and ⊙, respectively, stand for horizontal and vertical polarizations.

2.1.3. Polarizing beamsplitters (PBS)

These beamsplitters are two-input two-output devices for polarized light manipulations as can be seen in Fig.1. When the input photons to a PBS have the same polarization, PBS channels them to different outputs. On the other hand, when their polarizations are orthogonal, they are channelled to the same output. If we define an operator $\hat{R}_{PBS}$, then the action of the PBS on the inputs state can be summarized as $\hat{R}_{PBS}|1_V, 1_V\rangle = |1_V, 1_V\rangle$, $\hat{R}_{PBS}|1_H, 1_H\rangle = |1_H, 1_H\rangle$, $\hat{R}_{PBS}|1_V, 1_H\rangle = |0, 1_H 1_V\rangle$ and $\hat{R}_{PBS}|1_H, 1_V\rangle = |1_H 1_V, 0\rangle$. This property of PBS can be used as a parity checker which has very important consequences in entanglement purification schemes as we will discuss in the following sections.

2.1.4. Polarizers

A polarizer can be also named as polarization selector which allows the transmission of only one polarization state. The output polarization axis orientation is independent of the input polarization state. The plane of polarization is changed by rotating the linear polarizer about its optical axis. Two perfect polarizers with their transmission axes placed orthogonal to each other will extinguish the incident state.

2.1.5. Polarization Retarders

Another class of useful tools of linear optics for manipulating polarized light is the polarization retarders. Polarization manipulation is achieved in this device by introducing a relative phase between the orthogonal polarizations of the input field. There are two main retarders: Quarter wave plate (QWP) and half wave plate (HWP). A QWP, whose action on the polarization components of an input state of light is represented by the 2×2 matrix

$$\hat{R}_{QWP}(\theta) = \frac{1}{\sqrt{2}} \begin{pmatrix} 1 - i\cos(2\theta) & -i\sin(2\theta) \\ -i\sin(2\theta) & 1 + i\cos(2\theta) \end{pmatrix} \tag{5}$$

with θ being the angle between the input polarization and the fast axis of the retarder, is used to convert light between linear and circular polarization forms. It changes a linearly polarized light to a circular one if the angle between the input polarization and the fast axis of the retarder is $\theta = \pi/4$. Vertically and parallel polarized lights are converted, respectively, into right- and left-hand circularly polarized lights when $\theta = \pi/4$. An HWP whose 2×2 matrix representation reads as

$$\hat{R}_{HWP}(\theta) = -i \begin{pmatrix} \cos(2\theta) & \sin(2\theta) \\ \sin(2\theta) & -\cos(2\theta) \end{pmatrix} \tag{6}$$

rotates the input polarization by twice the angle, θ, between the input polarization and the fast axis of the device. A linearly polarized light remains a linearly polarized, except that the plane of polarization is rotated by 2θ . When θ is set to $\pi/4$, HWP converts a vertically polarized light into a horizontally polarized light. An HWP converts a right-hand circularly polarized light into a lef-hand circularly polarized light and vice versa, regardless of the angle θ. Polarization retarders can be used together with polarizers to construct variable polarization retarders, variable beamsplitters, variable attenuators and isolators.

2.1.6. Readout devices

Readout devices are necessary to characterize the output states at the end of an information processing task. In linear optics implementation of QIP, conditional measurement is required. That is the process is realized or a state is prepared only if some measurement outcomes are satisfied. These tasks require sophisticated readout and measurement devices. In linear optics toolbox, we have two main readout devices: photon counters and homodyne tomography. An ideal photon counter should resolve photon number incident on them with single photon resolution, have a very high quantum efficiency $\eta \sim 1$, a very low dark count rate $\nu \sim 0$, and no after pulsing. However, within the current level of technology these requirements cannot be met.

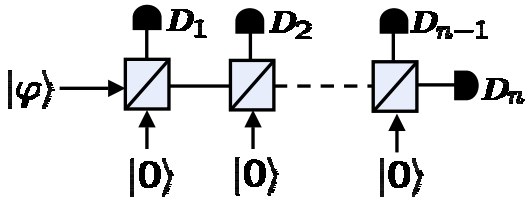

Figure 2. Schematic configuration of detection scheme with cascaded counters. $|\varphi\rangle$ denotes the input field to be detected and D_i represents the photon counters.

For a realistic description of photon-counting detectors, the positive-operator-valued measure (POVM) can be written as [5]

$$\Pi_N = \sum_{n=0}^{N} \sum_{m=n}^{\infty} \frac{e^{-\nu}\nu^{N-n}}{(N-n)!} \eta^n (1-\eta)^{m-n} C_n^m |m\rangle\langle m| \tag{7}$$

for a detector with quantum efficiency η (dead-time effects are included) and mean dark count of ν, where $\sum_{N=0}^{\infty} \Pi_N = 1$. In Eq.7, n and $N-n$ denote the actual number of photons present in the detection mode and the number of dark counts, respectively. N is the number of detected "clicks," and C_n^m is the binomial coefficient. Mean dark count rate is given by $\nu = \tau_{\rm res} R_{\rm dark}$, where $R_{\rm dark}$ is the dark count rate and $\tau_{\rm res}$ is the resolution time of the detector and the electronic circuitry. Currently, there are three photon counting schemes available and being used by different research groups:

Conventional photon counters: This type of counters employs avalanche photodiodes and can only distinguish the presence and absence of photons in the mode but cannot give any information on the exact number of photons in the mode when a detection event is registered. Therefore, such counters are usually referred to as ON/OFF detectors. They are available with dark count rates less than $100 s^{-1}$ and $\eta \sim 0.7$ [6]. POVM's for this type of detectors can be written as

$$\text{OFF} : \Pi_0 = \sum_{m=0}^{\infty} \mathrm{e}^{-\nu}(1-\eta)^m |m\rangle\langle m|, \quad \text{ON} : \ \Pi_{N\geq 1} = 1 - \Pi_0. \tag{8}$$

Single photon counters: This type of counters can discriminate no photon, a single photon and higher number of photons in the detection mode. They cannot distinguish two photons from higher number of photons. $\eta \simeq 0.7$ and dark count rates in the order of $10^4 s^{-1}$ have been reported [7]. POVM's for this type of detectors can be written as

$$\Pi_0 = \sum_{m=0}^{\infty} \mathrm{e}^{-\nu}(1-\eta)^m |m\rangle\langle m|, \ \ \Pi_1 = \sum_{n=0}^{1} \sum_{m=n}^{\infty} \mathrm{e}^{-\nu}\nu^{1-n}\eta^n m^n (1-\eta)^{m-n} |m\rangle\langle m|, \ \ \Pi_{N\geq 2} = 1 - \Pi_0 - \Pi_1. \tag{9}$$

Cascaded counters: Cascading conventional photon counters is a common way of solving the photon number discrimination problem. A schematic of this structure is shown in Fig.2. Principle is as follows: Lets assume that one has a system which can generate the correct output state when a single photon detection is registered at a photon counter. However, it is possible that $n > 1$ photons can fall on the counter which cannot resolve single photons. What one can do is to insert $(n-1)$ BS's on the light path and to keep the other inputs of all BS's at vacuum. Then photon counters are placed at the n outputs of the BS's. If only one of the detectors fires, the event is accepted; on the other hand if more than one of the detectors fire one can conclude that at the port to be measured there are more than one photon, and one does not consider it as a correct event. This advantage of this scheme comes with a high cost; that is the use of $(n-1)$ beamsplitters and n photon counters. Therefore, this technique is recommended only when the number of photons in a system is low.

Balanced homodyne tomography: Evaluation and verification of state preparation and manipulation tasks in the fields of quantum optics and QIP require the measurement of quantum states over all phase

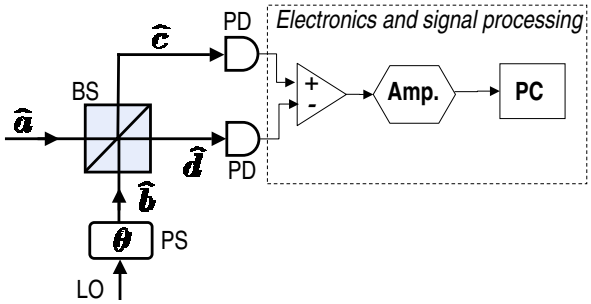

Figure 3. Basic scheme for balanced homodyne tomography. Signal state to be measured and the strong local oscillator (LO) are, respectively, in modes $\hat{a}$ and $\hat{b}$. BS is a symmetric, 50:50 beamsplitter. PD and Amp. stand for photodiode and amplifier, respectively. The phase θ is induced on the LO field by a phase shifter (PS).

space in order to obtain the exact information of the quantum state. Uncertainity principle tells us that it is impossible to make an exact measurement of both quadratures of a quantum state at the same time. However, balanced homodyne tomography (BHT) scheme can be used to reconstruct the Wigner function which contains all the information on the measured quantum state [8, 9]. The scheme is based on the direct measurement of quantum noise which is usually buried in the classical noise and very difficult to measure. However, in a BHT scheme, classical noise cancels out and measurement of the quantum noise becomes possible. BHT is composed of two main parts: the first part is the balanced homodyne detection to measure the quantum noise, and the second part is the signal processing part where the measured noise is processed using inverse Radon transform in order to construct the Wigner function of the quantum state under test.

The basic scheme of balanced homodyne tomography is shown in Fig. 3 where a signal field in mode $\hat{a}$ interferes with a strong local oscillator (LO) with amplitude α_{LO} in mode $\hat{b}$ at a 50:50 beamsplitter. LO phase is varied to take the projections of the quadratures at different angles. After the two light fields are mixed at the beamsplitter, the fields at the outputs of the beamsplitters are detected by photodiodes located at modes $\hat{c}$ and $\hat{d}$. The measured intensities at the detectors are subtracted from each other to obtain the difference intensity. The measured intensity at the detectors are related to the detected photon number, that is $I_c \propto \hat{n}_c = \hat{c}^\dagger \hat{c}$ and $I_d \propto \hat{n}_d = \hat{d}^\dagger \hat{d}$. Using the input-output relation for a 50:50 beamsplitter, we can write

$$\hat{n}_c = [\hat{n_a} + \hat{n_b} + \hat{a}^\dagger \hat{b} + \hat{b}^\dagger \hat{a}]/2, \qquad \hat{n}_d = [\hat{n_a} + \hat{n_b} - \hat{a}^\dagger \hat{b} - \hat{b}^\dagger \hat{a}]/2. \tag{10}$$

Then the intensity difference $\Delta I = I_c - I_d$ or the photon number difference $\Delta\hat{n} = \hat{n}_c - \hat{n}_d$ is found as $\Delta\hat{n} = \hat{a}^\dagger \hat{b} + \hat{b}^\dagger \hat{a}$. The strong LO condition enables us to replace the operators of the LO with c-numbers, that is we can use $\hat{b} = \alpha_{LO}$ and $\hat{b}^\dagger = \alpha^*_{LO}$ where α_{LO} can be represented as $\alpha_{LO} = |\alpha_{LO}|\ e^{i\theta}$. Then $\Delta\hat{n}$ becomes

$$\Delta\hat{n} = |\alpha_{LO}|[\hat{a}^\dagger\ e^{i\theta} + \hat{a}\ e^{-i\theta}] = \sqrt{2}|\alpha_{LO}|\hat{q}_\theta, \tag{11}$$

where $\hat{q}_\theta$ is the phase dependent quadrature. $\Delta\hat{n}$ can be normalized by $\sqrt{2}|\alpha_{LO}|$ to make it independent of the LO intensity. Therefore, it becomes clear that balanced homodyne scheme measures the quadrature distribution at a projection phase provided by the LO. In an experimental realization, the modulation of the LO phase is achieved by a mirror mounted on a piezoelectric transducer or by electro-optical modulator (EOM). Repeating measurements at a fixed LO phase gives the statistics and distribution of quadratures. LO phase then is scanned at equal intervals between 0 to π and different projection distributions are obtained. In this way, $f(x, \theta)$ which is the probability distribution of the measured quadrature after a phase shift θ is collected.

After $f(x, \theta)$ is collected, the signal processing stage starts. In this stage, $f(x, \theta)$ is first filtered and then the output is sum up over all projection angles θ. Indeed, this process corresponds to Inverse Radon Transform which is written as

$$W(q, p) = \frac{1}{2\pi^2} \int_0^\pi d\theta \int_{-\infty}^{\infty} dx f(x, \theta) K(q\cos\theta + p\sin\theta - x), \tag{12}$$

where the $K(...)$ is a Kernel function or the filtering function. This function has some practical obstacles: (i) it is singular, and (ii) in practice a filter has a limited bandwidth, that is, limits of integration cannot be from $-\infty$ to $+\infty$. Therefore a regularization is needed when dealing with $K(...)$. This is done by setting a cutoff frequency k_c as the integration limits. Then in the implementation, it is considered as a piecewise-function

$$K(y) = \begin{cases} \frac{k_c^2}{2}[1 - \frac{k_c^2 y^2}{4} + \frac{k_c^4 y^4}{72}...] & \text{if } |k_c y| \leq 0.1 \\ \frac{x}{y} & \text{if } |k_c y| > 0.1 \end{cases} \tag{13}$$

The choice of k_c is very important and it must be optimized for each specific experiment. Choosing high values causes high frequency fluctuations, on the other hand, low values may cause the loss of some characteristic properties of the Wigner function by smoothing out it.

Lastly, we point out that BHT scheme does not need photon counters with single photon resolution but rather use photodiodes for measuring the current. The following points should be satisfied for a successfull implementation of BHT: (i) strong LO, (ii) spatial and time-frequency mode-match of the state to be measured and the LO, (iii) balanced (to cancel out classical noise components) and stable (to prevent fluctuations in the phase) interferometer: (iv) photodiodes with high detector efficiency, (v) low electrical noise (must be much lower than the shot noise which reflects the fluctuations of the light intensity), (vi) high amplification over a large bandwidth.

2.1.7. Auxiliary photons: single photons from parametric down conversion process

In order to prepare quantum states of arbitrary structures, we need to use auxiliary photons and coherent light. Here we will briefly review the generation of single photons and the current level of technology in the area. Preparing single photon states are important not only because we can use them as auxiliary photons, but also because we can study the fundamentals of quantum optics using these highly nonclassical states of light. However, it is very difficult to prepare single photons, because it requires the generation of exactly one and only one photon with energy in a well-defined spectra and spatial mode. At present, spontaneous parametric down conversion (SPDC) process is the most widely used method to prepare single photon states. Besides SPDC, recently there has been successful demonstration of single photon sources using quantum dot technology. However, at present they are not as common as the SPDC in usage. Therefore, we restrict ourselves to a detailed analysis of SPDC as a single photon source in this section.

In SPDC process, two photons (denoted as idler and signal) with lower energy are generated when a nonlinear crystal is pumped with a strong pump laser as seen in Fig.4. The probability of having this down conversion is very small. Conservation of energy fixes the frequencies of the generated photons via $\hbar\omega_p = \hbar\omega_i + \hbar\omega_s$ where p,i, and s correspond to pump, idler and signal, respectively. However, due to the finite size of the nonlinear crystal, the photons may have broader bandwidths, even if the pump light has narrow bandwidth. Therefore, a spectral filtering is needed to obtain photons with well-defined spectrums. Emission directions of these photons are determined with the conservation of momentum as $\overrightarrow{k}_p = \overrightarrow{k}_i + \overrightarrow{k}_s$. The photons are emitted in a cone of radiation, and hence their location in the cone is important. Photons with well-defined spatial modes can be obtained by using spatial filtering with apertures. The two photons created in this way are highly entangled in energy, momentum, time, polarization, phase and photon number under appropriate conditions. Even though, the photons in the idler and signal modes do not enjoy a well-defined phase of their own, their phase is related to the phase of the pump field through $\phi_p = \phi_i + \phi_s$. The expression for the output of a SPDC process may be written as [10]

$$|\varphi\rangle_{(i,s)} = \sqrt{1-\gamma^2}\sum_0^\infty (\gamma e^{i\phi_p})^n |n\rangle_i |n\rangle_s, \tag{14}$$

where γ^2 is the rate of one-photon pair generation and is typically $\mathcal{O}(10^{-4})$ [11], n is the number of photons generated in pairs in the idler and signal modes, and θ_p is the phase of the pump field.

There are two types of SPDC characterized according to the relation between the polarizations of the emitted photons which is determined by the crystal and the polarization of the pump field [12]. In type I process, the generated photons have the same polarization whereas in the type II process they have orthogonal polarizations (see Fig. 5). One who wants to use SPDC as a single photon source should keep in mind that

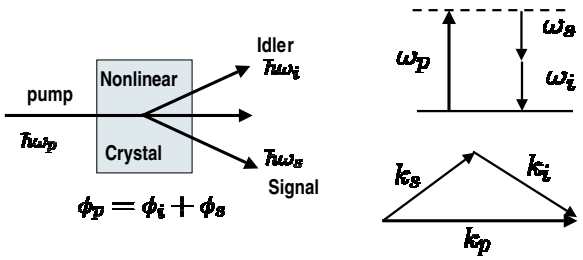

Figure 4. Schematic illustration of spontaneous parametric down conversion (SPDC). $\hbar$,ω,ϕ and k stand for the Planck's constant, angular frequency, phase and the wavevector of the fields in SPDC.

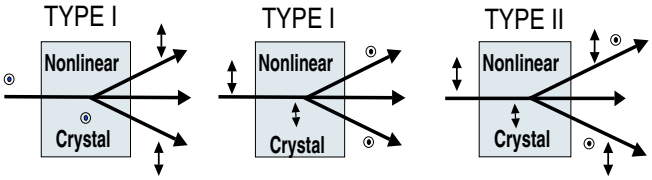

Figure 5. Polarization properties of the photon pairs generated in type I and type II SPDC.

(i) the photon pairs are generated at random times, (ii) most of the time it is the vacuum at the output of the process, (iii) even though the probability is much lower, there may be cases where more than one photon pair is generated. Therefore, to use SPDC for this purpose, one should use a conditional measurement, that is, when a detector placed in idler mode registers a "click", there is photon in the signal mode as schematically shown in Fig. 6 (left). In practice, this technique suffers from detector inefficiencies discussed in the former section, that is, the commercially available detectors do not resolve single photons. A "click" registered with such detectors does not necessarily mean that there is only one photon in the output, there might be more than one photon. An experimental characterization of single photons generated by conditional measurement from a SPDC using balanced homodyne tomography has been performed by Lvovsky et al.[13].

3. Qubit state generation

In this section, we present some of the theoretical proposals and experiments which utilize linear optics toolbox for optical qubit state generation:

3.1. Qubit encoded in polarization

A qubit encoded in the polarization degree of freedom of a single photon can be constructed by placing polarization retarders on the signal mode of SPDC. As it can be seen from Eq.6, a single HWP can prepare only linearly polarized states in which the relative weights of the vertical and horizontal polarizations can be adjusted by the rotation angle θ of the HWP. Circular and elliptical states can be prepared using a single QWP (see Eq.5). Indeed, particular polarization changes on a single photon can be implemented by passing it through a HWP, or a QWP, or a HWP and QWP placed one after another. In order to make arbitrary changes on the polarization state of a single photon to produce arbitrary qubit states, the configuration seen in Fig.6 (right), where a HWP is placed between two QWP's, is needed.

3.2. States generated by displacement and photon adding

In this subsection, we introduce the schemes based on displacement and photon adding aoperators. These operators can be used alone or together in various ways to prepare nonclassical states of light.

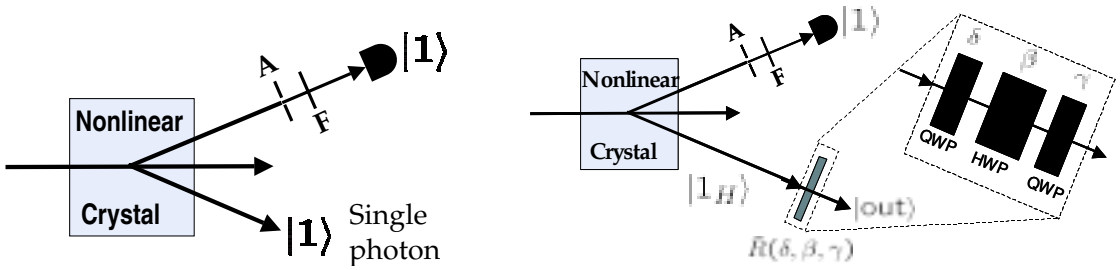

Figure 6. Preparation of single photon (left) and qubit state encoded in polarization degree of freedom of a photon (right) using SPDC. $\hat{R}(\delta,\beta,\gamma)$ stands for the polarization rotation induced by the combined half-wave plate (HWP) and quarter-wave plates (QWP's) which is shown in the dotted box. δ, β, and γ are the angles between the input polarization and the fast axis of the retarders. A and F represent aperture and narrowband interference filter, respectively.

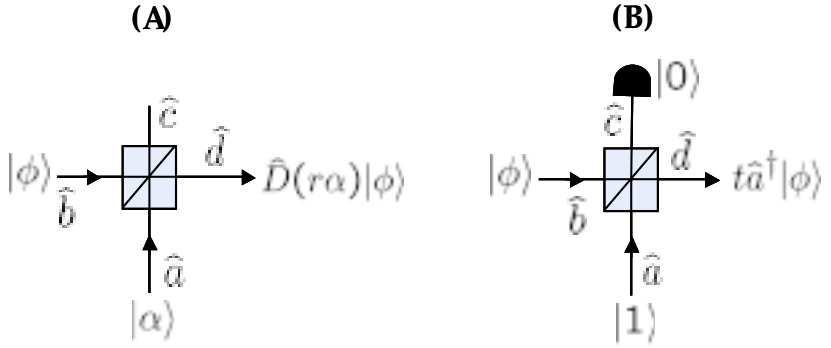

Figure 7. Schemes for (A) displacementent and (B) photon adding operators.

Displacement operator is defined as $\hat{D}(\alpha) = \exp(\alpha\hat{a}^\dagger - \alpha^*\hat{a})$ with α being the amount of displacement. A coherent state $|\alpha\rangle$ can be generated by applying $\hat{D}(\alpha)$ on vacuum state that is $|\alpha\rangle = \hat{D}(\alpha)|0\rangle$, where α denotes the amplitude of a coherent state. It has been shown that $\hat{D}(\alpha)$ can be physically realized by a beamsplitter with $r \ll 1$ shown in Fig.7(A) where no measurement is needed at the other output port of the BS, and $|\phi\rangle$ is an arbitrary state.

Photon adding, too, can be achieved by using a BS. In this case, a single photon $|1\rangle$ and an arbitrary state $|\phi\rangle$ are fed into the BS as seen in Fig.7(B). If the state at the output mode-$\hat{d}$ is conditioned on no-photon detection in mode-$\hat{c}$, the state at mode-$\hat{d}$ reduces onto $t\hat{a}^\dagger|\phi\rangle$ from which it is seen that a photon is added to the state $|\phi\rangle$.

3.2.1. Displaced Fock state:

Displaced Fock states, which were theoretically described by Boiteux and Levelut [14], are highly nonclassical states. A Fock state does not carry any phase information, whereas as we will see a displaced Fock state carries a phase information. This makes displaced Fock state a very useful tool for probing the phase relations. It has been shown that quasidistribution of any quantum state can be represented as a series of displaced Fock states [15, 16, 17]. Displaced Fock states can be generated by applying a displacement operator on a Fock state as shown in Fig.7(A) if $|\phi\rangle$ is replaced by a Fock state $|m\rangle$. Then the output of BS becomes

$$|\text{out}\rangle = \frac{1}{\sqrt{m!}}\hat{D}_c(t\alpha)\hat{D}_d(r\alpha)(t\hat{d}^\dagger + r\hat{c}^\dagger)^m|0\rangle_c|0\rangle_d. \tag{15}$$

If no measurement is done at mode-$\hat{c}$, the state at mode-$\hat{d}$ becomes $|\phi\rangle_d = \hat{D}_d(r\alpha)|m\rangle$ provided that $r \ll 1$. It is now clear that the output state is a Fock state carrying the phase information of the coherent state

through $\alpha = |\alpha|e^{i\theta}$ where θ is the phase of the coherent light. An experimental demonstration of displaced Fock state generation has been performed by Lvovsky et al. [18] where linear optics toolbox has been used. Tomographic reconstruction of the prepared states shows the nonclassical properties of these states clearly.

3.2.2. Superposition States

The simplest of superposition states is $c_0|0\rangle + c_1|1\rangle$ (with proper normalization) can be generated using displacement operator followed by a conditional measurement. If the input coherent state in Fig.7A satisfies $\alpha \ll 1$, that is, it can be expanded as $|\alpha\rangle \simeq |0\rangle + \alpha|1\rangle$, and we select the events where one and only one photon is detected at a detector placed on mode-$\hat{c}$ output of the BS, the state at the other output of the BS becomes $|\text{out}\rangle_d = \mathcal{N}(t|0\rangle + \alpha|1\rangle)$ where $\mathcal{N}^{-2} = |t|^2 + |\alpha|^2$ [19, 20].

Superposition states with arbitrary finite dimension $|\phi\rangle = \sum_n c_n|n\rangle$ can be prepared from a vacuum state by alternate applications of displacement and photon-adding operators as shown in Fig.8 [19]. At the first stage labelled as "displacement" and bounded with a dotted box in Fig.8, a vacuum state $|0\rangle$ and a strong coherent light $|\alpha_1\rangle$ are mixed at the first beamsplitter whose transmittance is very close to unity. This corresponds to the displacement operator and creates a coherent state $|r_1\alpha_1\rangle = \hat{D}(r_1\alpha_1)|0\rangle$. At the second stage inside the dotted box labelled as "photon adding", a single photon addition is performed by superimposing the $|r_1\alpha_1\rangle$ with $|1\rangle$ on the condition that no photon is detected at the other output port of this second beamsplitter. This will generate the state $t_2\hat{a}^\dagger|r_1\alpha_1\rangle = t_2\hat{a}^\dagger\hat{D}(r_1\alpha_1)|0\rangle$. In the next step, these two stages are repeated whose effect can be easily seen by replacing $|\alpha_1\rangle$ by $|\alpha_2\rangle$. Then the state at the output of the fourth beamsplitter will become $t_4\hat{a}^\dagger\hat{D}(r_2\alpha_2)t_2\hat{a}^\dagger\hat{D}(r_1\alpha_1)|0\rangle$. Repeating this procedure N times, and at the end applying the last displacement $\hat{D}(\alpha_{N+1})$ complete the task of generating arbitrary finite dimensional superposition states. To generate a state with desired coefficients c_n, one should be careful in choosing the beamsplitter transmittance in the photon adding stage and the intensity of the input coherent state in the displacement stage. This scheme has not been experimentally demonstrated.

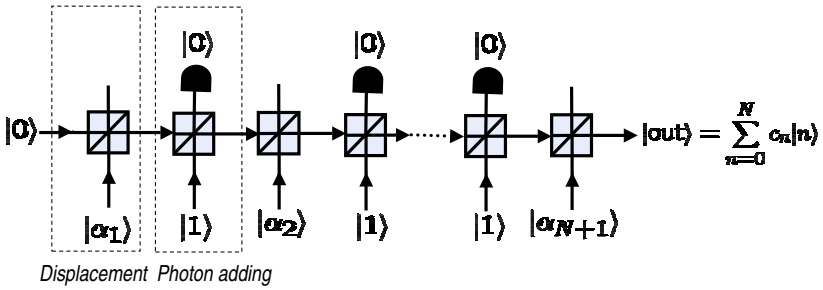

Figure 8. Basic scheme for generating arbitrary superposition states using alternate displacement and photon adding.

3.3. Teleportation based qubit state preparation

Quantum scissors device (QSD) is a scheme for preparing superposition states based on the concept of teleportation [21, 22, 23, 24]. In this scheme the superposition state is prepared by truncating a coherent state which is expressed in photon number basis as

$$|\alpha\rangle = e^{-|\alpha|^2/2}\sum_{n=0}^{\infty}\frac{\alpha^n}{\sqrt{n}}|n\rangle = e^{-|\alpha|^2/2}[|0\rangle + \alpha|1\rangle + \frac{\alpha^2}{\sqrt{2}}|2\rangle....]. \tag{16}$$

To prepare the qubit state only the part of the coherent state up to a specific photon number is teleported to a spatially separated place, e.g., teleportation of only the part of to one photon state that is $\mathcal{N}[|0\rangle + \alpha|1\rangle]$ with $\mathcal{N}$ is a renormalization factor. The originally proposed basic scheme of the QSD and the scheme for its practical realizations are given in Fig. 9. It must be noted that no light from the input coherent state $|\alpha\rangle$ reaches to the output state $|out\rangle$, so this process is a nonlocal process relying on entanglement. The

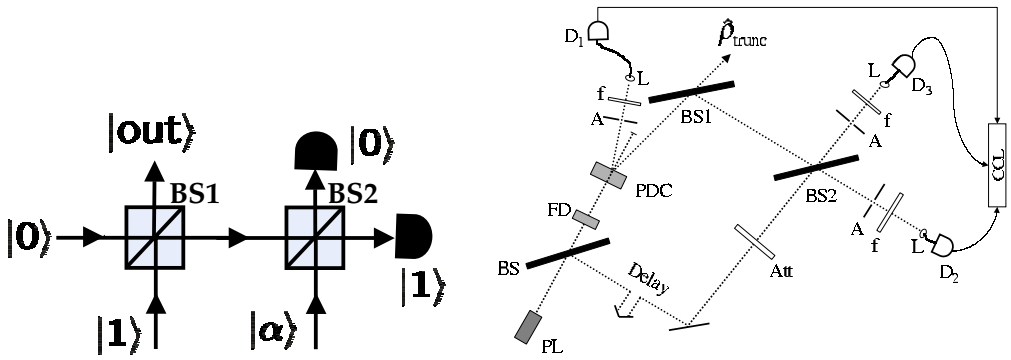

Figure 9. Basic scheme of quantum scissors device (left) and the scheme for its experimental realization (right). PL, pulsed laser; FD, frequency doubler; PDC, parametric down conversion crystal; Att, strong attenuator; A, aperture; f, narrow band filter; L, lens; CCL, coincidence counter and logic; BS, BS1, and BS2 are beam splitters; and D_1, D_2, and D_3 are photon-counting detectors.

entangled state is produced at BS1 (50:50) by mixing $|0\rangle$ and $|1\rangle$. The Bell measurement which is the essential element of teleportation scheme is performed by BS2 (50:50) and two photon counters placed at its output ports. A detection event of $|0\rangle$ and $|1\rangle$ at the photon counters teleports and truncates the input coherent state $|\alpha\rangle$ to $c_0|0\rangle + c_1|1\rangle$ with proper normalization. In other detection events, the protocol fails to generate the desired output state. The scheme can be extended to generate superposition states of the form $\mathcal{N}[|0\rangle + \alpha|1\rangle + \frac{\alpha^2}{\sqrt{2}}|2\rangle]$ as follows: Beamsplitters BS1 and BS2 are chosen as $|r_1|^2 = |r_2|^2 = 0.21$ or $|r_1|^2 = |r_2|^2 = 0.79$, the inputs of the BS1 are now both $|1\rangle$, and the required measurement result is $|1\rangle$ and $|1\rangle$ at the detectors [25]. The weights of vacuum and one-photon state in the superposition can be varied or tuned to desired values either by proper choice of beam-splitter parameters or by adjusting α [26, 27]. This basic scheme cannot be used to extend the output state to higher dimensions.

QSD, as we have already mentioned, performs both teleportation and truncation, therefore, it can be used as a teleporter for superposition states without making any change [25, 28]. If one wants to teleport a state $c_0|0\rangle + c_1|1\rangle$, first he/she can prepare it with the QSD scheme with the input $|\alpha\rangle$. Then this output superposition state of the first QSD can be fed into a second QSD as the input and perform the teleportation process when vacuum and one-photon are registered at the detectors. The same is valid for preparing and teleporting $c_0|0\rangle + c_1|1\rangle + c_2|2\rangle$.

4. Bell state preparation using SPDC

Entangled states and their joint measurement in the basis of four maximally entangled states, which are referred to as Bell states or EPR pairs, form an essential part of QIP schemes. These states can be prepared using the polarization entangled photon pairs created by SPDC. Four Bell states which can be unitarily transformed to each other are written as

$$\begin{aligned} |\Phi^{\mp}\rangle &= \frac{1}{\sqrt{2}}(|HH\rangle \mp |VV\rangle) \\ |\Psi^{\mp}\rangle &= \frac{1}{\sqrt{2}}(|HV\rangle \mp |VH\rangle). \end{aligned} \tag{17}$$

In the non-collinear type-II SPDC process where the photons are created in orthogonal polarizations, at certain angles between the pump-beam and the optic axis of the crystal, the photons are emittted in cones which do not have a common axis. While one of these cones has horizontally polarized photons, the other will have vertically polarized photons. Along the intersection of these cones, one cannot distinguish whether a certain photon is vertically or horizontally polarized provided that the "walkoff", which is caused by different group velocities of the horizontally and vertically polarized light in the crystal, is compensated. This compensation can be usually done by inserting birefringent crystals, e.g. quartz of various thickness in

each of the beam paths. When the compensation is achieved, the state can be described as

$$|\Psi\rangle \quad = \quad \frac{1}{\sqrt{2}}(|HV\rangle + e^{i\varphi}|VH\rangle) \tag{18}$$

where the angle φ can be adjusted by using compensator crystals [29]. By using a HWP in one of the beam paths, we can transform the $|\Psi^{\mp}\rangle$ into $|\Phi^{\mp}\rangle$.

Another way of generating Bell states is to use two nonlinear crystal geometry either in type-II [30] or type-I [31] SPDC. Fig.10 shows the idea for type-I process. In this scheme, the crystals are stacked to each other in such a way that their optic axis are perpendicular to each other. Then if the pump beam is chosen as a linearly polarized light at 45°, in the first crystal, horizontally polarized portion of the pump beam creates a horizontally polarized photon pair, whereas in the second crystal the vertically polarized portion creates a vertically polarized photon pair. If the "walkoff" effect is compensated using additional crystals, the resultant state becomes

$$|\Phi\rangle \quad = \quad \frac{1}{\sqrt{2}}(|HH\rangle + e^{i\varphi}|VV\rangle) \tag{19}$$

from which other Bell states can be prepared by using a HWP and a QWP.

An essential part of a quantum communication scheme is a Bell state analyzer. Indeed, there is a large number of QIP applications, such as teleportation [1], dense coding [2], quantum repeaters [32] and fault tolerant quantum computing [33], where it is needed to project an incoming state on to the Bell state. When a two-photon state is input, a Bell state analyzer determines which one of the Bell states the input is. The basic principle of a Bell state analyzer is that only one of the Bell states, $|\Psi^{-}\rangle$, given in Eq.(17) is anti-symmetric while the other three are symmetric under the exchange of particles. If we define four modes two of which correspond to internal state that is the polarization (V,H), and the other two correspond to external state that is the spatial modes (a,b), then the Bell states can be written as

$$|\Psi\rangle^{\mp} = \frac{1}{\sqrt{2}}(\hat{a}_H^{\dagger}\hat{b}_V^{\dagger} \mp \hat{a}_V^{\dagger}\hat{b}_H^{\dagger})|0\rangle, \qquad |\Phi\rangle^{\mp} = \frac{1}{\sqrt{2}}(\hat{a}_H^{\dagger}\hat{b}_H^{\dagger} \mp \hat{a}_V^{\dagger}\hat{b}_V^{\dagger})|0\rangle. \tag{20}$$

Let's assume that any of these Bell states is incident symmetrically on a 50:50 BS. Then the output of the BS denoted by the spatial modes c and d becomes as follows for each of the input state:

$$\begin{aligned}
|\Psi^{-}\rangle &\rightarrow \frac{1}{\sqrt{2}}(|1_H\rangle_c|1_V\rangle_d + |1_V\rangle_c|1_H\rangle_d) \\
|\Psi^{+}\rangle &\rightarrow \frac{i}{\sqrt{2}}(|2_{H,V}\rangle_c|0\rangle_d + |0\rangle_c|2_{H,V}\rangle_d) \\
|\Phi^{+}\rangle &\rightarrow \frac{i}{2\sqrt{2}}(|2_H\rangle_c + |2_V\rangle_c)|0\rangle_d + |0\rangle_c(|2_H\rangle_c + |2_V\rangle_c) \\
|\Phi^{-}\rangle &\rightarrow \frac{i}{2\sqrt{2}}(|2_H\rangle_c - |2_V\rangle_c)|0\rangle_d + |0\rangle_c(|2_H\rangle_c - |2_V\rangle_c).
\end{aligned} \tag{21}$$

It is seen that if the incident state is a symmetric Bell state then two photons emerge together in one of the two outputs of BS. On the contrary, in case of the antisymmetric state, $|\Psi^{-}\rangle$, one photon is present at each output mode of BS leading to a coincidence detection if photon counters are placed at the output of the BS. Therefore, it can be said that $|\Psi^{-}\rangle$ can be discriminated from the other three Bell states by a coincidence detection at the output of a 50:50 BS [34, 35]. But this is not enough for a Bell state analyzer. A further analysis of the symmetric Bell states shows that only the state $|\Psi^{+}\rangle$ has different polarizations for each photon. Therefore, making a polarization measurement at the output of 50:50 BS can allow us distinguish the $|\Psi^{+}\rangle$ from the other two states $|\Phi^{\mp}\rangle$. This polarization measurement is done by inserting PBS at each output of the 50:50 BS and using four photon counters placed at the output of PBS's. If a coincidence detection is registered at the output of one of the PBS's, then the incoming state is $|\Psi^{+}\rangle$, on the other hand, if one photon is detected at the output of one of the PBS and another photon at the output of the other PBS is detected, then the input state is $|\Psi^{-}\rangle$. All other cases correspond to $|\Phi^{\mp}\rangle$. In this way a Bell state analyzer with 50% efficiency can be realized. Here, we must note that there is a No-go theorem which states that never failing complete Bell state analyzer is impossible using only linear optics toolbox [36].

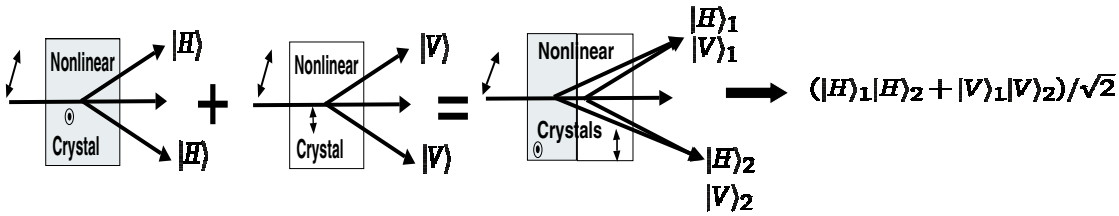

Figure 10. Bell state preparation using type-I SPDC with two nonlinear crystals stacked together with their optics axes orthogonal to each other.

5. Entanglement Extraction

Entanglement is a very specific and precious resource in QIP applications such as teleportation, dense coding and secure key distribution. On the other side, it is a source of hard to overcome problems in QIP. However, quantum information community has come up with very clear ways of dealing with such problems and manipulating entangled states.

One of the main problems related with entangled states emerges in the distribution of these states. Since entanglement cannot be created by local operations alone, entanglement should be distributed, at some point, between the spatially separated parties to build up non-local quantum correlations. During the distribution process, these qubits will unavoidably interact with the channel (environment) which will induce decoherence reducing the purity of the entangled state and resulting in some mixed state which is less-entangled than the original one. To overcome this problem *entanglement extraction* protocols, which are used to extract from a large number of less-entangled states a smaller number of more-entangled states, have been proposed [37, 38, 39]. Based on these protocols, experimentally feasible schemes have been proposed [40, 41, 42, 43]. In these protocols, the spatially separated parties are restricted to use LOCC (Local Operation and Classical Communication). Because it is only in this restriction that the parties are forced to use the less-entangled states they have in order to generate a smaller number states with higher entanglement. In LOCC, one of the parties, say Alice, can use any unitary operator, von Neumann or any generalized measurement only on the Hilbert space of her particles. She cannot manipulate the particles of the other party, Bob, neither can they exchange particles or any quantum system. Recently, LOT has been successfully exploited for entanglement extraction and practical realization of proposed protocols[44, 45, 46, 47].

5.1. Protocols for entanglement extraction

Schmidt Projection Method: This is originally proposed for the concentration of entanglement of pure partially entangled states [37]. The method takes its name from the projection of the joint state of n-particles onto a subspace spanned by eigenstates of the reduced density operator, $\hat{\rho}_A$ (or $\hat{\rho}_B$) of a bipartite pure state $|\varphi\rangle_{AB}$, with the same eigenvalues. Hence, it correponds to the number of terms in the Schmidt decomposition of $|\varphi\rangle_{AB}$ which is expressed as

$$|\varphi\rangle_{AB} = \sum_i c_i |\alpha_i\rangle_A |\beta_i\rangle_B \tag{22}$$

with c_i being real and positive, and $\{\alpha_i\}$ and $\{\beta_i\}$ forming orthonormal states of subsystem A and B, respectively. Now, let us assume that Alice and Bob share n of partially entangled pure states $|\varphi\rangle_{AB} = \lambda_0|HH\rangle + \lambda_1|VV\rangle$ with $|\lambda_0|^2 + |\lambda_1|^2 = 1$. Then the complete state of the particles they share can be written as

$$\Psi_n = \bigotimes_{j=1}^{n} |\varphi\rangle_{AB} = \sum_{k=0}^{n} \lambda_0^k \lambda_1^{n-k} \{|H^{\otimes k} V^{\otimes(n-k)}\rangle_A |H^{\otimes k} V^{\otimes(n-k)}\rangle_B\} \tag{23}$$

where the states in curly brackets denote the sum of all states with having k number of H. For example, $\{|H^{\otimes 2}V^{\otimes 1}\rangle_A |H^{\otimes 2}V^{\otimes 1}\rangle_B\}$ stands for $|HHV\rangle_A|HHV\rangle_B + |HVH\rangle_A|HVH\rangle_B + |VHH\rangle_A|VHH\rangle_B$. Then defining the unnormalized state $|\chi_k\rangle_A|\chi_k\rangle_B = \{|H^{\otimes k}V^{\otimes(n-k)}\rangle_A|H^{\otimes k}V^{\otimes(n-k)}\rangle_B\}$, Eq.(23) becomes

$\Psi_n = \sum_{k=0}^{n} \lambda_0^k \lambda_1^{n-k} |\chi_k\rangle_A |\chi_k\rangle_B$. Here we define $|\varphi_k\rangle = |\chi_k\rangle_A |\chi_k\rangle_B$ which is unnormalized, and write $\Psi_n = \sum_{k=0}^{n} \lambda_0^k \lambda_1^{n-k} |\varphi_k\rangle$ from which it is seen that the set $\{|\varphi_k\rangle\}$ forms orthogonal basis and all $|\varphi_k\rangle$ are maximally entangled. Then with a probability $\binom{n}{k}|\lambda_0|^{2k}|\lambda_1|^{2(n-k)}$, Alice and Bob get a maximally entangled state $|\varphi_k\rangle$ with an amount of entanglement equals to $E(|\varphi_k\rangle) = \log_2 \binom{n}{k}$. They can do that if Alice counts the number of $|H\rangle$'s in the joint space of n qubit they share. Now the problem of Alice and Bob is reduced to transforming the state they have into the product of Bell states. In order to do this, first they have to use a function which performs the mapping $\{\chi_k\} \rightarrow \{0, 1, 2, ..., \binom{n}{k}\}$, e.g. for $n = 3$ and $k = 2$, $|HHV\rangle_A |HHV\rangle_B + |HVH\rangle_A |HVH\rangle_B + |VHH\rangle_A |VHH\rangle_B \rightarrow |0\rangle_A |0\rangle_B + |1\rangle_A |1\rangle_B + |2\rangle_A |2\rangle_B$. Then using this mapping and defining $\delta_k = \binom{n}{k}$,

$$|\varphi_k'\rangle = \frac{1}{\sqrt{\delta_k}} \sum_{j=0}^{\delta_k - 1} |j\rangle_A |j\rangle_B \tag{24}$$

can be written. Each of j is a binary string with length $L_k = \log_2 \binom{n}{k}$. If δ_k is a power of 2, then the state $|\varphi_k'\rangle$ is a product of L_k Bell pairs. For example, lets assume that they share $n = 4$ partially entangled pairs and they make their measurement and keep the states with $k = 3$, that is states with three $|H\rangle$. Then with probability $4|\lambda_0|^6|\lambda_1|^2$, they will have a maximally entangled state from which they can extract two Bell (EPR) pairs. The state $|\varphi_3\rangle$ is obtained as

$$\begin{aligned} |\varphi_3\rangle &= |\chi_3\rangle_A |\chi_3\rangle_B \\ &= |HHHV\rangle_A |HHHV\rangle_B + |HHVH\rangle_A |HHVH\rangle_B + |HVHH\rangle_A |HVHH\rangle_B + |VHHH\rangle_A |VHHH\rangle_B \\ &\rightarrow |\varphi_3'\rangle = \frac{1}{2}(|0\rangle_A |0\rangle_B + |1\rangle_A |1\rangle_B + |2\rangle_A |2\rangle_B + |3\rangle_A |3\rangle_B). \end{aligned} \tag{25}$$

Then in binary form of two bits $L_j = 2$, $|\varphi_3'\rangle$ becomes

$$|\varphi_3'\rangle = \frac{1}{2}(|00\rangle_A |00\rangle_B + |01\rangle_A |01\rangle_B + |10\rangle_A |10\rangle_B + |11\rangle_A |11\rangle_B). \tag{26}$$

Keeping in mind that $\delta_j = 4$ is a power of 2, different bits of the binary string are disentangled, therefore we can directly write

$$\begin{aligned} |\varphi_3'\rangle &= \frac{1}{2}(|00\rangle_{AB} + |11\rangle_{AB})(|00\rangle_{AB} + |11\rangle_{AB}) \\ &= \frac{1}{2}(|HH\rangle_{AB} + |VV\rangle_{AB})(|HH\rangle_{AB} + |VV\rangle_{AB}) = |\Phi^+\rangle|\Phi^+\rangle \end{aligned} \tag{27}$$

where we labelled $|0\rangle \rightarrow |H\rangle$ and $|1\rangle \rightarrow |V\rangle$.

The problem becomes more complicated for Alice and Bob if δ_k is not a power of two. Now let's assume that it is either a power of two or slightly higher than a power of two, that is $2^{L_k} \leq \delta_k < 2^{L_k+1}$. Then they can measure the most significant bit (MSB) of the qubits they have when it is written in the binary form. With a probability $2^{L_k}/\delta_k$, they will obtain a zero. In this case the state will collapse to a subspace of 2^{L_k}, then they can extract L_k pairs by taking the bits $L_0, L_1, ..., L_{k-1}$ where L_k denotes the MSB. However, if δ_k is much higher than a power of two, then there still exists a problem for them and they can solve the problem by repeating the above protocol. What they do is as follows: They take another batch of n samples and make measurement. Let us assume that this time they obtain the state $|\varphi_{k_1}'\rangle$. Then the new dimension of the combined state of the first batch and the second batch becomes $\binom{n}{k}\binom{n}{k_1}$. They check whether this satisfies $2^\ell \leq \delta < 2^\ell(1+\epsilon)$ for some ℓ and predetermined ϵ. If this is the case, then they are happy because they can split the dimension into two orthogonal subspaces, one of which is dimension 2^ℓ and the other with $L - 2^\ell$. Then they can write their states in binary form and measure the MSB as explained above to extract ℓ pairs. If not, they have to take new batches and repeat the procedure until they obtain a combined state dimension that satisfies the above inequality.

A schematic description of the Schmidt projection method is illustrated in Fig.11. This method for entanglement manipulation requires at least $n = 2$ non-maximally entangled pure states. The efficiency increases with increasing n. Alice and Bob need not know the exact states of the shared pairs they start

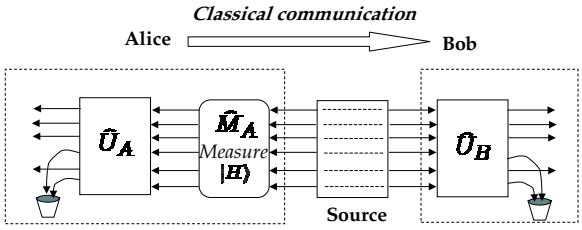

Figure 11. Schematic diagram of Schmidt projection method. Source generates non-maximally entangled pairs. Alice performes a non-destructive measurement on her qubits and pass the measurement result to Bob via classical communication channel. Based on this measurement, they apply a unitary operator to transform their states into the one they want and then throw away the unwanted pairs.

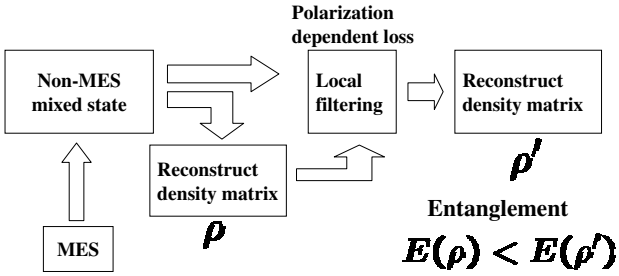

Figure 12. Schematic diagram of local filtering protocol. The exact state of the non-maximally entangled state (non-MES) ρ is determined first. Based on this measurement, polarization dependent losses are set and purification process starts. A tomography of the state after filtering, ρ', can be done to reconstruct its density operator from which the amount of entanglement represented as $E(\rho')$ can be calculated.

with; however, the pairs should be identical. The difficulty in the implementation is the need for non-destructive measurement which is not available with the current level of technology and the tools to operate collectively on a large number of photons.

Local Filtering (Procrustean Method): This method is especially suitable for increasing the entanglement of pure states [37]. This method works for individual pairs and does not need collective manipulation of pairs. Using this method, a pure state of the form

$$|\varphi\rangle = \lambda_0|HH\rangle + \lambda_1|VV\rangle, \tag{28}$$

which is a non-maximally entangled state with $\lambda_0 \neq \lambda_1$ being two real numbers and satisfying $\lambda_0^2 + \lambda_1^2 = 1$, can be transformed into the maximally entangled state $|\Phi^+\rangle$ by introducing polarization dependent absorbers or reflectors (coated glass slabs or Brewster window) on one or both of the qubits. If we assume that $\lambda_0 > \lambda_1$, this filtering operation with polarization dependent losses should be designed either to cut down the value of λ_0 to equalize it at λ_1, or to cut down both of them to have a value λ which is less than λ_0 and λ_1. Then Alice and Bob can use the filters with the following transmission matrices

$$T_A = T_B = \begin{pmatrix} \sqrt{\lambda_1/\lambda_0} & 0 \\ 0 & 1 \end{pmatrix}, \tag{29}$$

which attenuates the horizontally polarized light. Then the output qubits, that is the qubits which pass these filters, is the maximally entangled state, $|\Phi^+\rangle$. If the qubits are absorbed then Alice and Bob declares the failure of the process. It is easy to see that Alice and Bob keeps the output filtered state $|\Phi^+\rangle$ with a probability $2|\lambda_1|^2$, and discard the qubits with probability $1 - 2|\lambda_1|^2$. Thus this nonunitary filtering process equalizes the contribution of the two terms in Eq.28 yielding a perfect entanglement. This process

is also applicable to the cases where the initial state is partially mixed in addition to being non-maximally entangled. The drawback of this method is that exact state of of the qubit pair should be known by Alice and Bob to customize the polarization dependent losses, without this information losses to be inserted cannot be decided. Then Alice and Bob should make a tomographic measurement to understand the exact state of the qubit pairs, assuming that, the pairs they receive are all identical. Then based on this measurement they set the losses and apply filtering on the new non-maximally and mixed states. A schematic configuration which summarizes local filtering is depicted in Fig. 12. This method of entanglement extraction has been experimentally realized by Kwiat et al. [44].

Recurrence Method: This protocol works for two-qubit states whose fidelity to a Bell state is $\mathcal{F} > 1/2$ [38]. Assuming Alice and Bob share n identical $\hat{\varrho}$ states with fidelity $\mathcal{F}$, the protocol proceeds as follows: **(1)** Alice chooses an independent, random SU(2) operator $\hat{U}$ for each state and applies it to her particles. Then she tells the operators she has chosen to Bob who applies $\hat{U}^*$ to his particles. This operation which is called as "Twirling" transforms the original general mixed state into a Werner state

$$W = F|\Psi^-\rangle\langle\Psi^-| + \frac{1-F}{3}(|\Psi^+\rangle\langle\Psi^+| + |\Phi^-\rangle\langle\Phi^+| + |\Phi^+\rangle\langle\Phi^+|) \tag{30}$$

in which the weight of $|\Psi^-\rangle$ is the highest, "mostly $|\Psi^-\rangle$". The effect of the twirling operation is diagonalization of the mixed state in the Bell basis without changing its fidelity to $|\Psi^-\rangle$. **(2)** Alice performs a σ_y operation on her qubits. This operation transforms $|\Psi^-\rangle$ into $|\Phi^+\rangle$. **(3)**Using their two states as control and target states, Alice and Bob perform bilateral quantum controlled-NOT (C-NOT) operation which is referred to as (BXOR). An important feature of BXOR is that it maps Bell states into Bell states. A complete table showing how the BXOR operates can be found in Ref.[38]. The reason for step 2 is clear when the truth table for BXOR is analyzed. When a $|\Phi^+\rangle$ is used as the control and target states for the BXOR, the resultant control and target states do not change. **(4)** The pair of target qubits is then measured locally. Then they exchange their results (two-way classical communication). If their results are different, they discard both the target and control states. Otherwise, they keep the control state. By applying this test, Alice and Bob are able to distinguish $|\Psi^\mp\rangle$ from $|\Phi^\mp\rangle$ the latter of which gives the same result for Alice and Bob. **(5)** Alice performs a σ_y operation to transform the state to a mostly $|\Psi^-\rangle$ state which has a greater $\mathcal{F}$ than the starting state. **(6)** Alice and Bob repeat the steps 1-5 to increase the fidelity until they obtain a $\mathcal{F}$ which is high enough for their purpose. The relation between the fidelities after and before the purification process is given as

$$\mathcal{F}' = \frac{\mathcal{F}^2 + (1/9)(1-\mathcal{F})^2}{\mathcal{F}^2 + (2/3)\mathcal{F}(1-\mathcal{F}) + (5/9)(1-\mathcal{F})^2} \tag{31}$$

where $\mathcal{F}$ is the fidelity of the states entering the purification process and $\mathcal{F}'$ is the fidelity of the remaining state after the purification.

Recurrence method basically repeats the cycle: σ_y-BXOR-measurement-σ_y. If the starting state is Werner state in which the weight of $|\Psi^-\rangle$ is high, each cycle makes the coefficient of $|\Psi^-\rangle$ higher so that the Werner state will become closer to $|\Psi^-\rangle$. For this to be performed, Alice and Bob do not have to know exactly the state they start with. In order to know which qubits to keep and which ones to discard, Alice and Bob needs a two-way communication. The drawbacks of this method can be listed as follows: (i) It is not very efficient because in order to get a pair very close to a maximally entangled state, a high number of these processes should be repeated, and in the limit of very high fidelity, that is an exact Bell pair, the yield approaches to zero, (ii) with the current level of technology, two qubit BXOR operation is difficult to perform in practice.

The scheme works as long as $F > 1/2$ for all states, which may not be identical. In a recent work, Pan et al., has performed an experimental realization of this protocol starting from a mixed state of the form $\hat{\varrho} = F|\Psi^+\rangle\langle\Psi^+| + (1-F)|\Phi^-\rangle\langle\Phi^-|$ using only linear optics toolbox [47].

5.2. Experimental realization of entanglement extraction based on Schmidt projection method

The first ever successful entanglement extraction experiment using a collective operation on photon pairs was performed in our group at SOKENDAI by Yamamoto et al. [45] based on a simple theoretical scheme

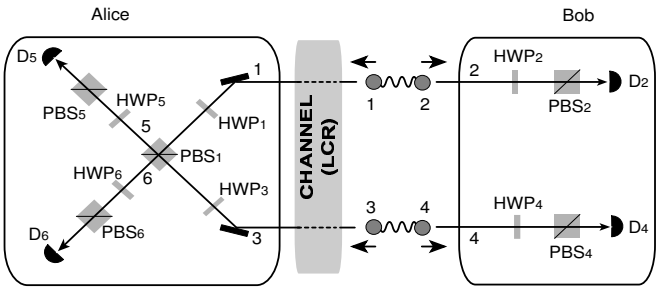

Figure 13. Schematic diagram of the experimental setup. The channel realized by a a liquid crystal retarder (LCR) is a phase damping channel which gives identical phase fluctuations to photons in mode 1 and 3. (HWP_2, PBS_2, D_2) and (HWP_6, PBS_6, D_6)are used only for the verification of the extracted photon pair at modes 2 and 6. HWP_1 is inserted for an auxiliary experiment and it is not relevant here for an additional π phase shift.

derived from the original Schmidt projection method. In this section, we will briefly introduce the theoretical background and then present the experimental results.

The scheme, which is depicted in Fig.13, works as follows [42, 45]: Let us assume that we have a source which prepares partially entangled pure states in the form $|\psi\rangle_{12} = \alpha|HH\rangle_{12} + \beta|VV\rangle_{12}$ and $|\psi\rangle_{34} = \alpha|HH\rangle_{34} + \beta|VV\rangle_{34}$ where α and β are complex numbers satisfying $|\alpha|^2 + |\beta|^2 = 1$. Alice receives the photons in modes 1 and 3, whereas Bob receives the photons in modes 2 and 4. The complete state of these pairs can be written as

$$\begin{aligned} |\psi\rangle_{12}|\psi\rangle_{34} &= (\alpha|HH\rangle_{12} + \beta|VV\rangle_{12}) \otimes (\alpha|HH\rangle_{34} + \beta|VV\rangle_{34}) \\ &= \alpha^2|HH\rangle_{13}|HH\rangle_{24} + \beta^2|VV\rangle_{13}|VV\rangle_{24} + \alpha\beta(|HV\rangle_{13}|HV\rangle_{24} + |VH\rangle_{13}|VH\rangle_{24}) \end{aligned} \quad (32)$$

which is a superposition of separable states with coefficients α^2 and β^2, and an entangled state with the coefficient $\alpha\beta$. Then the task is to discard the first two terms (separable part) and extract a maximally entangled pair from the last terms (more entangled part) using LOCC. Since the partially entangled states that Alice and Bob share are identical, they can apply Schmidt projection method to extract a maximally entangled pair of the form $|\Phi^+\rangle$. This can be done as follows: Alice makes a collective non-destructive polarization measurement which gives the number of vertically polarized photons. If the outcome is one, she communicates the result to Bob and they keep the state which now becomes $|HV\rangle_{13}|HV\rangle_{24}+|VH\rangle_{13}|VH\rangle_{24}$. Then they can apply local unitary operator to obtain $|\Phi^+\rangle$. The essential point here is the nondestructive measurement which determines the polarization of each photon without destroying it. However, this is not possible with the current technology. Instead, Alice and Bob can use linear optics toolbox and perform destructive measurement with photon counters to achieve the same task: **(1)** Alice rotates the polarization of the photon in mode 3 by $\pi/2$ using a HWP_3. This will make the transformation $|H\rangle_3 \rightarrow |V\rangle_3$ and $|V\rangle_3 \rightarrow |H\rangle_3$. **(2)** The output of HWP_3 is sent to PBS_1 whose other input is the photon coming in mode 1. After the PBS_1, the complete state becomes

$$\alpha^2|H\rangle_6|V\rangle_6|H\rangle_2|H\rangle_4 + \beta^2|V\rangle_5|H\rangle_5|V\rangle_2|V\rangle_4 + \alpha\beta(|H\rangle_5|H\rangle_6|H\rangle_2|V\rangle_4 + |V\rangle_5|V\rangle_6|V\rangle_2|H\rangle_4). \quad (33)$$

It is seen that by counting the number of photons in mode 5 we can discard the unwanted parts. The desired part which contains the expressions with coefficient $\alpha\beta$ is selected if and only if there is one photon in mode 5. This one photon can be in either of the polarizations, therefore the measurement process should not distinguish $|H\rangle$ from $|V\rangle$. **(3)** Alice measures the incoming photons on the diagonal basis $\{|D\rangle_5, |\overline{D}\rangle_5\}$ and Bob measures on $\{|D\rangle_4, |\overline{D}\rangle_4\}$ where $|D\rangle = (|H\rangle + |V\rangle)\sqrt{2}$ and $|\overline{D}\rangle = (|H\rangle - |V\rangle)\sqrt{2}$ for both modes 4 and 5. **(4)** If Alice measures one photon on $|D\rangle_5$ and Bob measures one photon on $|D\rangle_4$, then the modes 2 and 6 share the Bell state $|\Phi^+\rangle$. **(5)** By communicating their measurement results via classical communication channel, Alice and Bob can extract a Bell pair.

In our experiments, polarization entangled photons are generated using the method described in Sect.4 (Fig.10) by SPDC collinearly [31, 42]. Then the photons are separated by a beamsplitter inserted on their

path. The nonlinear crystals used in the experiment are β-barium borate (BBO). After the first entangled pair is generated, the pump beam is reflected back passing the crystals in the opposite direction generating the second entangled pair. Here, once more, we have to note that this process generates entangled photon pairs in a nondeterministic way. The failures due to component losses, channeling effect of the beamsplitters and no photon generation in either or both of the crystals can be discarded by post-selection. That is, the events when four detectors register photon detection (four-fold coincidence detection) will be considered as the successful events, other cases will be discarded.

After the photon pairs are generated, one photon from each pair is sent to Alice through a channel which induces a time varying random phase shift. The two photons are launched into the channel within the correlation time of the phase fluctuations of the channel in order to ensure that they are affected with identical phase fluctuations. This phase damping channel is realized using a liquid crystal retarder (LCR) which can change the phase between $|H\rangle$ and $|V\rangle$ proportional to the applied voltage. The phase is varied between 0 and π in eight intervals for 10s. At the end of this phase damping, the state of the ensemble of each pair becomes

$$\begin{aligned} \rho_{12} &= \frac{1}{2}(|HH\rangle_{12}\langle HH| + |VV\rangle_{12}\langle VV|) \\ \rho_{34} &= \frac{1}{2}(|HH\rangle_{34}\langle HH| + |VV\rangle_{34}\langle VV|) \end{aligned} \tag{34}$$

where the off-diagonal elements are averaged out and the pairs are no longer entangled. In order to show this is really the case in our experiments, we measured the correlations between the polarizations of photons in each pair, separately, both before and after the phase fluctuations are induced. Polarization correlations were probed by making two-fold coincidence measurements. For example, for the photon pair in modes 3 and 4, coincidence counts at detectors D_4 and D_5 were recorded for various angles of HWP_3 and HWP_4 while the photons in modes 1 and 2 were blocked and the HWP_5 was adjusted so that it does not rotate the polarization. For the pair in modes 1 and 2, the same measurements were performed for various angles of HWP_1 and HWP_2 while the photons in modes 3 and 4 were blocked and HWP_6 was adjusted so that it does not rotate the polarization. The results of these measurements are given in Table 1 and Fig.14 for the pair in mode 3 and 4. From the table, it is seen that $|HH\rangle_{34}$ and $|VV\rangle_{34}$ are dominant. The coherence between these terms should show up as an interference fringe in the count rate of D_4 when HWP_4 is rotated on the condition that a photon is detected in mode 3. It is seen that the visibility of the interference curve is 0.89 before the LCR is modulated (no phase fluctuation) implying the presence of highly entangled photon pairs. When the phase fluctuations are introduced as above by modulating the LCR, the visibility of the interference curve became less than 0.03 which is a sign of the loss of coherence. By making tomographic measurement, we reconstructed the density matrix for the decohered pair and calculated the entanglement of formation to be very small $\simeq 0.0018$. These results clearly indicated that our source for photon pair generation and the realization of the phase damping channel worked as expected. Moreover, we see that when each pair is considered individually after the channel, there is almost no entanglement. As we have discussed above, using this scheme which is based on collective manipulation of photon pairs, Alice and Bob can extract a highly entangled photon pair if the detectors D_4 and D_5 register photons. Since our source is not a deterministic source, we have to make post-selection, hence a four-fold coincidence detection at detectors D_2, D_4, D_5 and D_6. This will automatically discard the events where there are two photons in mode 5 (no photon in mode 6). In Fig.14 (C), we present the result of the polarization correlation measurements for photons in mode 2 and 6 conditioned on coincidence detection at detectors D_4 and D_5.

The visibility of the interference curve is found to be 0.63 ± 0.05 which is well above the achievable value of 0.5 in the classical model. Then the lower bound for the fidelity of the extracted entangled state in modes 2 and 6 to a maximally entangled state $|\Phi^-\rangle$ is calculated to be 0.78 ± 0.05. Then from this lower bound of fidelity, the lower bound for the entanglement of formation of the extracted pair is calculated as 0.42 ± 0.12. Thus the extracted pair in this experiment is clearly shown to be entangled. The visibility of the interference curve and hence the amount of entanglement extracted in this experiment is limited mainly due to residual temporal and spatial mode mismatch between the photons belonging to different pairs.

Table 1. Rates of coincidence detection on $\{|H\rangle, |V\rangle\}$ basis before decoherence, after decoherence, and after the extraction process. $|HH\rangle$ and $|VV\rangle$ are dominant. The coherence of these terms are probed by making measurement along the diagonal basis as shown in Fig.14.

	HH	HV	VH	VV
Before decoherence (10s)	15230	118	244	15173
After decoherence (80s)	121189	1225	2016	118858
After extraction (9600s)	109	5	4	116

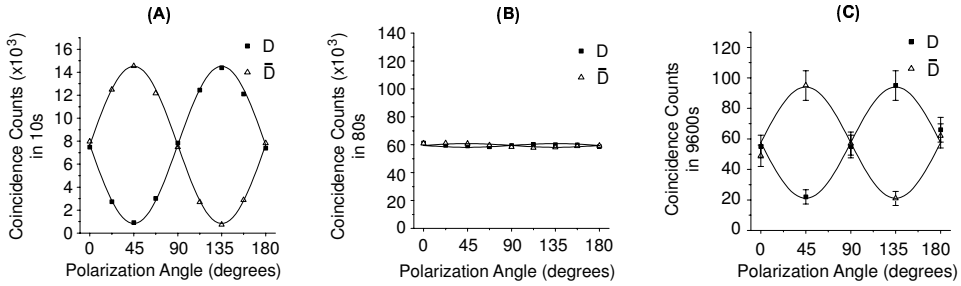

Figure 14. Results of photon correlation measurements for three important stages of the experiments. (A) Testing the entanglement of the photon pair generated by the SPDC source used in the experiment. This measurement was performed while the LCR was kept unmodulated (no phase fluctuation). (B) Verification of the decoherence of the individual photon pairs when one photon from each pair passes through the LCR while the LCR is modulated (phase fluctuations are induced). Coherence is lost. Coincidence events rate where a photon in polarization $|D\rangle$ is detected at D_5 and a linearly polarized photon with angle θ is detected at D_4 are shown. During these measurements modes 1 and 2 were blocked. (C) Verification of the entanglement of the extracted pair after the collective manipulation of two photons. Coincidence events where a photon in polarization $|D\rangle$ (or $|\overline{D}\rangle$) is detected at D_6 while a linearly polarized photon with polarization angle θ is detected at D_2 on the condition that D_4 and D_5 both register a photon. The error bars assume Poisson statistics and the solid curves represent the best fit to the data. $\theta = 0$, $\theta = \pi/4$, $\theta = \pi/2$, $\theta = 3\pi/4$, respectively correspond to $|H\rangle$, $|D\rangle$, $|V\rangle$, and $|\overline{D}\rangle$.

6. Results and Conclusions

In this review paper, we have shown that LOT contains powerful tools that can enable the realization of fundamental requirements for QIP applications. Although we have restricted ourselves for the review of qubit state generation and entanglement extraction, LOT has been shown both theoretically and experimentally to be applicable in quantum gate construction, as well [48, 49, 50, 51]. The most important restrictions on LOT applications come from more fundamental problems in single photon counting and generation. However, the recent developments and ongoing successful works on these counters and sources give us the hope that such problems will be overcome in near future. Therefore, there waits new and exciting fields to be explored using those new equipments within the linear optics toolbox.

Acknowledgements

Ş. K. Özdemir thanks Dr. T. Hakioglu, Dr. T. Yıldırım, Dr. O. Gülseren and Dr. Z. Gedik for their invitation and hospitality during the QCAS 2003 summer school.

References

[1] C.H. Bennett, G. Brassard, C. Crepeau, R. Jozsa, A. Peres, and W.K. Wootters, *Phys. Rev. Lett.,* **70**, (1993), 1895.

[2] C.H. Bennett and S.J. Wiesner, *Phys. Rev. Lett.,* **69**, (1992), 2881.

[3] R.A. Campos, B.E.A. Saleh, and M.C. Teich, *Phys. Rev. A,* **40**, (1989), 1371.

[4] M.S. Kim, W. Son, V. Buzek, and P.L. Knight, *Phys. Rev. A,* **65**, (2002), 032323.

[5] S.M. Barnett, L.S. Phillips, and D. T. Pegg, *Opt. Commun.* **158**, (1998), 45.

[6] Data sheet on SPCM-AQ photon-counting module, EG&G, Optoelectronics Division, Vaudreuil, Canada.

[7] J. Kim, S. Takeuchi, Y. Yamamoto, and H.H. Hogue, *Appl. Phys. Lett.* **74**, (1999), 902.

[8] D.T. Smithey, M. Beck, M.G. Raymer, and A. Faridani, *Phys. Rev. Lett.* **70**, (1993), 1244; D.G. Welsch, W. Vogel, and T. Opatrný, in *Progress in Optics*, edited by E. Wolf (North-Holland, Amsterdam, 1999), Vol. 39, p. 63, and references therein.

[9] U. Leonhardt, *Measuring the Quantum State of Light* (Cambridge), (1997).

[10] B. Yurke and M. Potasek, *Phys. Rev. A,* **36**, (1987), 3464; D.R. Truax, *Phys. Rev. D* **31**, (1985), 1988.

[11] D. Bouwmeester et al., *Nature (London),* **390**, (1997), 575; D. Bouwmeester, J.-W. Pan, H. Weinfurter, and A. Zeilinger, *J. Mod. Opt.* **47**, (2000), 279.

[12] P.G. Kwiat, Ph.D. Thesis, University of california at Berkeley, 1993; A. Garuccio, Ann. N.Y. Acad. *Sci.* **755**, (1995), 632.

[13] A.I. Lvovsky, H. Hansen, T. Aichele, O. Benson, J. Mlynek, and S. Schiller *Phys. Rev. Lett.,* **87**, (2001), 050402.

[14] M. Boiteux and A. Levelut, *J. Phys. A* **6**, (1973), 589.

[15] K.E. Cahill, R.J. Glauber, Phys. Rev. **177**, 1857 (1969); **177**, (1969), 1882.

[16] A. Wünsche, *Quantum Opt.* **3**, (1991), 359.

[17] H. Moya-Cessa and P.L. Knight, *Phys. Rev. A,* **48**, (1993), 2479.

[18] A. I. Lvovsky and S. A. Babichev, *Phys. Rev. A,* **66**, (2002), 011801(R).

[19] M. Dakna, J. Clausen, L. Knöll, and D. G. Welsch, *Phys. Rev. A,* **59**, 1658 (1999), and references therein.

[20] A.I. Lvovsky and J. Mlynek, *Phys. Rev. Lett.,* **88**, (2002), 250401.

[21] D.T. Pegg, L.S. Phillips, and S.M. Barnett, *Phys. Rev. Lett.,* **81**, (1998), 1604.

[22] S.M. Barnett and D.T. Pegg, *Phys. Rev. A,* **60**, (1999), 4965.

[23] Ş. K. Özdemir, A. Miranowicz, M. Koashi, and N. Imoto *Phys. Rev. A,* **64**, (2001), 063818.

[24] Ş. K. Özdemir, A. Miranowicz, M. Koashi, and N. Imoto *Phys. Rev. A,* **66**, (2002), 053809.

[25] M. Koniorczyk, Z. Kurucz, A. Gabris, and J. Janszky, *Phys. Rev. A,* **62**, (2000), 013802.

[26] M. G. A. Paris, *Phys. Rev. A,* **62**, (2000), 033813.

[27] Ş. K. Özdemir, A. Miranowicz, M. Koashi, and N. Imoto J. Mod. Opt., **49**, (5/6), (2002), 977.

[28] C.J. Villas-Bôas, N.G. de Almeida, and M. H. Y. Moussa, *Phys. Rev. A,* **60**, (1999), 2759 .

[29] P.G. Kwiat, K. Mattle, H. Weinfurter, A. Zeilinger, A. V. Sergienko and Y. Shih, *Phys. Rev. Lett.,* **75**, (1995), 4337.

[30] P.G. Kwiat, E. Waks, A.G. White, I. Appelbaum, and P.H. Eberhard, *Phys. Rev. A,* **60**, (1999), R773R776.

[31] Y.H. Kim, S.P. Kulik, and Y. Shih, *Phys. Rev. A,* **62**, (2002), 011802.

[32] H.-J. Briegel, W. Dur, J.I. Cirac, and P. Zoller, *Phys. Rev. Lett.,* **81**, (1998), 593

[33] D. Gottesman and I.L. Chuang, *Nature,* **402**, (1999), 390.

[34] N. Lütkenhaus, J. Calsamiglia, and K.A. Suominen, *Phys. Rev. A,* **59**, (1999), 3295.

[35] M. Michler, K. Mattle, H. Weinfurter, and A. Zeilinger, *Phys. Rev. A,* **53**, (1996), R1209.

[36] J. Calsamiglia, N. Lütkenhaus, *Appl. Phys. B,* **72**, (2001), 67.

[37] C.H. Bennett, G. Brassard, S. Popescu, B. Schumacher, J.A. Smolin, and W.K. Wootters, *Phys. Rev. Lett.,* **76**, (1996), 722.

[38] C.H. Bennett, H.J. Bernstein, S. Popescu, and B. Schumacher, *Phys. Rev. A,* **53**, (1996), 2046.

[39] C.H. Bennett, D.P. DiVincenzo, J.A. Smolin, and W.K. Wootters, *Phys. Rev.,* A **54**, (1996), 3824.

[40] S. Bose, V. Vedral, and P.L. Knight, *Phys. Rev. A*, **60**, (1999), 194.

[41] J.-W. Pan, C. Simon, C. Brukner, and A. Zeilinger, *Nature (London),* **410**, (2001), 1067.

[42] T. Yamamoto, M. Koashi, and N. Imoto, *Phys. Rev. A*, **64**, (2001), 012304.

[43] Z. Zhao, J.-W. Pan, and M. S. Zhan, *Phys. Rev. A,* **64**, (2001), 014301.

[44] P.G. Kwiat, S. Barraza-Lopez, A. Stefanov, and N. Gisin, *Nature (London),* **409**, (2001), 1014.

[45] T. Yamamoto, M. Koashi, Ş.K. Özdemir, and N. Imoto, *Nature (London),* **421**, (2003) 343.

[46] Z. Zhao, T. Yang, A.-N. Zhang, and J.-W. Pan, *Phys. Rev. Lett.,* **90**, (2003), 207901.

[47] J.-W. Pan, S. Gasparoni, R. Ursin, G. Weihs, and A. Zeilinger, *Nature (London),* **423**, (2003), 417.

[48] E. Knill, R. Laflamme, and G.J. Milburn, *Nature (London)*, **409**, (2001), 46.

[49] M. Koashi, T. Yamamoto, and N. Imoto, *Phys. Rev. A,* **63**, (2001), 030301.

[50] T.B. Pittman, B.C. Jacobs, and J.D. Franson, *Phys. Rev. A,* **66**, (2002), 052305.

[51] T.B. Pittman, B.C. Jacobs, and J.D. Franson, *Phys. Rev. Lett.,* **88**, (2002), 257902.